Cell, Vol. 114, 75–86, July 11, 2003, Copyright ©2003 by Cell Press

Differential Control of the Releasable Vesicle Pools by SNAP-25 Splice Variants and SNAP-23

Jakob B. Sørensen,[1,4,*] Gábor Nagy,[1,4] Frederique Varoqueaux,[2] Ralf B. Nehring,[1] Nils Brose,[2] Michael C. Wilson,[3] and Erwin Neher[1]

[1] Max-Planck-Institute for Biophysical Chemistry
Am Fassberg 11
37077 Göttingen
Germany

[2] Max-Planck-Institute for Experimental Medicine
Hermann-Rein-Strasse 3
37075 Göttingen
Germany

[3] Department of Neurosciences
University of New Mexico Health Sciences Center
Albuquerque, New Mexico 87131

Summary

The SNARE complex, consisting of synaptobrevin, syntaxin, and SNAP-25, is essential for calcium-triggered exocytosis in neurosecretory cells. Little is known, however, about how developmentally regulated isoforms and other cognate SNARE components regulate vesicular fusion. To address this question, we examined neuroexocytosis from chromaffin cells of *Snap25* null mice rescued by the two splice variants SNAP-25a and SNAP-25b and the ubiquitously expressed homolog SNAP-23. In the absence of SNAP-25, vesicle docking persisted, but primed vesicle pools were empty and fast calcium-triggered release abolished. Single vesicular fusion events showed normal characteristics, except for a shorter duration of the fusion pore. Overexpression of SNAP-25a, SNAP-25b, and SNAP-23 resulted in three distinct phenotypes; SNAP-25b induced larger primed vesicle pools than SNAP-25a, whereas SNAP-23 did not support a standing pool of primed vesicles. We conclude that three alternative SNARE components support exocytosis, but they differ in their ability to stabilize vesicles in the primed state.

Introduction

Synchronization of exocytosis with electrical activity in excitable cells is made possible by the tight temporal linkage between vesicle fusion and the intracellular calcium signal. This feature of neuroexocytosis depends on (1) the presence of a pool of release-ready or "primed" vesicles, formed by maturation of vesicles already docked to the plasma membrane (Parsons et al., 1995), and (2) the steep dependency of the fusion probability of primed vesicles on the intracellular calcium concentration, $[Ca^{2+}]_i$ (Dodge and Rahamimoff, 1967). Recent evidence suggests that the Ca^{2+}- and phospholipid binding function of synaptotagmin I is likely to form the basis for the calcium sensor for exocytosis (e.g. Mackler et al., 2002; Shin et al., 2003). The question remains, however, what is the molecular basis for the formation of the primed pool of vesicles?

The neuronal SNARE complex is formed between SNARE proteins residing in the vesicle membrane (synaptobrevin) and the plasma membrane (syntaxin and SNAP-25), linking the membranes together to promote fusion (Jahn and Südhof, 1999; Chen and Scheller, 2001). SNAP-25 contributes two α helices to the total of four that constitute the SNARE complex (Sutton et al., 1998) and is anchored in the membrane by palmitoylation of four cysteines residing in the "linker" region between the two SNARE motifs (Vogel and Roche, 1999). Alternative splicing of exon 5 gives rise to two isoforms, SNAP-25a and -25b (Bark and Wilson, 1994), which differ by nine amino acids, including six amino acids in the N-terminal SNARE motif and three amino acids in the linker region, altering the position of one of the palmitoylated cysteines. The SNAP-25a isoform is more abundant in the embryonic mouse brain and in adult neurosecretory cells; however, the SNAP-25b isoform becomes the dominating form in brain after birth during the major period of synaptogenesis (Bark et al., 1995). Despite subtle biochemical differences (Puffer et al., 2001) and the possibility to induce isoform-specific expression (Hepp et al., 2001), it has been difficult to distinguish physiological differences between the isoforms in neuroexocytosis (Gonelle-Gispert et al., 1999). SNAP-23 is a homolog of SNAP-25 (58% identity on the amino acid level), with an almost ubiquitous expression pattern (Ravichandran et al., 1996; Wang et al., 1997). Similarly to SNAP-25, SNAP-23 is localized to the plasma membrane (Wang et al., 1997) and can form a SNARE complex with synaptobrevin 2 and several syntaxin isoforms (Ravichandran et al., 1996). Thus, at least three distinct proteins seem able to play the role of SNAP-25 in the exocytotic SNARE complex, raising the questions how alternative splicing of SNAP-25 may affect Ca^{2+}-triggered exocytosis and whether the more generalized SNAP-23 containing SNARE complex can substitute for the neuronal SNARE complex. Resolving these issues should extend our understanding of how constitutive and more specialized forms of exocytosis are distinguished and regulated in different cell types.

In the present study, we have made use of the *Snap25* knockout mouse to investigate vesicle secretion from fetal chromaffin cells using rapid electrophysiological techniques under conditions where either SNAP-25 isoform alone or SNAP-23 participated in secretion. Our data show that all three SNARE proteins can support vesicular fusion and neurotransmitter release; however, the distinguishing feature of the SNAP-25 isoforms is that they are able to support a standing pool of primed vesicles. In this respect, the SNAP-25b isoform is two to three times more efficient than the SNAP-25a isoform.

Results

Embryos deficient in SNAP-25, hence referred to as mutants, were generated by crossing heterozygous parent

*Correspondence: jsoeren@gwdg.de
[4] These authors contributed equally to this work.

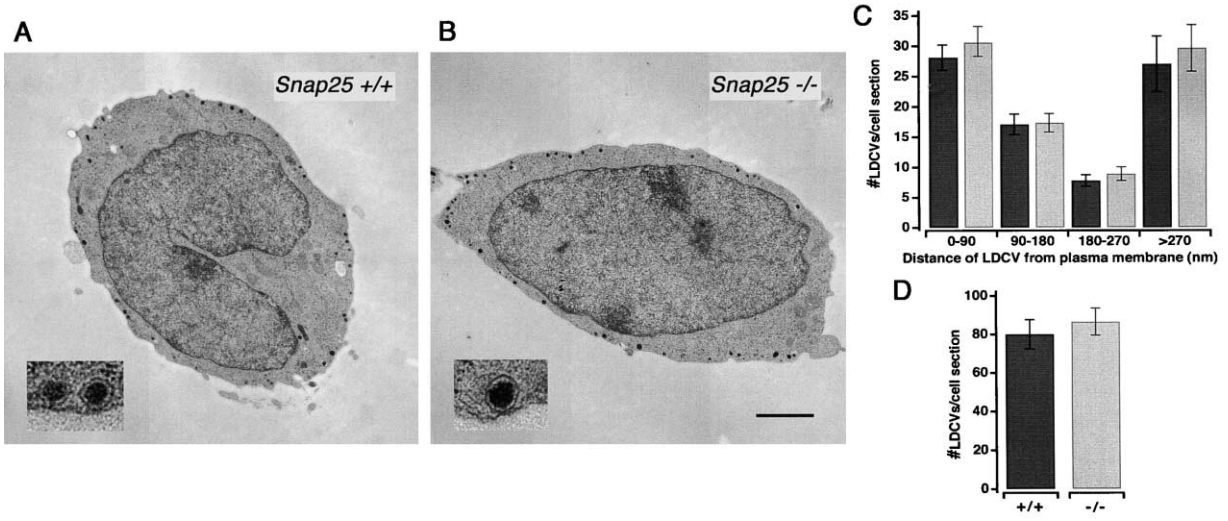

Figure 1. Normal Docking of Large Dense-Core Vesicles in the Absence of SNAP-25

(A and B) Electron micrographs of isolated chromaffin cells from wild-type (*Snap25*$^{+/+}$, [A]) and SNAP-25 mutant (*Snap25*$^{-/-}$, [B]) animals. In both cell types, most vesicles were found along the plasma membrane. Insets: closeup of docked vesicles. Scale bar: 1.45 μm (190 nm for insets).

(C) The distributions (mean ± SEM) of distances between the center of chromaffin granules and the plasma membrane (wild-type cells: black bars, n = 30 cells from three animals; mutant cells: gray bars, n = 27 cells from three animals) showed no defect in docking in the absence of SNAP-25. Note that we measured the distance from the center of the granules; the membrane-to-membrane distances were even smaller.

(D) Total number of vesicles per cell section (mean ± SEM) in wild-type (black bars) and mutant (gray bars) cells.

animals and recovered by caesarean section at embryonic day (E)18 (Washbourne et al., 2002). Using an enzymatic method (Experimental Procedures), we prepared isolated embryonic chromaffin cells in parallel from mutant, heterozygous, and homozygous wild-type littermates.

Ultrastructure of SNAP-25 Mutant Cells

It is generally accepted that in neuroexocytosis, docking of vesicles to the plasma membrane is a prerequisite for priming and, ultimately, fusion. Since trans-SNARE complexes could provide a mechanism for directing docking of vesicles to their appropriate target membranes (Söllner et al., 1993), we first investigated by electron microscopy whether large dense-core vesicles (LDCVs) were morphologically docked in the absence of SNAP-25. As previously described for embryonic mouse chromaffin cells (Voets et al., 2001b), a large proportion of vesicles were found aligned with the plasma membrane in homozygous wild-type cells (Figure 1A). Analysis of homozygous SNAP-25 mutant cells demonstrated that these vesicles also were located very close to the plasma membrane (Figure 1B). As a quantitative index of morphological docking, we measured the distance from the center of the vesicles to the plasma membrane in wild-type and mutant cells. No significant difference was found either for the distribution (Figure 1C) or the total number of vesicles per cell section (Figure 1D), indicating that SNAP-25 is not required for normal morphological vesicle docking.

Stimulation by Flash Photolysis of Caged Ca^{2+}

In order to investigate the exocytotic process, we performed whole-cell patch clamp on isolated chromaffin cells. The cells were loaded with a calcium cage (nitrophenyl-EGTA) and calcium-sensitive dyes through the pipette, and secretion was evaluated simultaneously by capacitance measurements and amperometry. Stimulation of chromaffin cells by flash photolysis of caged Ca^{2+} typically causes a biphasic increase in membrane capacitance (control traces in Figures 2A and 2B). The first phase, the exocytotic burst, lasts for approximately 0.5 s after the flash and can be further subdivided into a fast burst (fusion with time constant ~20 ms at 20 μM Ca^{2+}) and a slow burst (fusion with time constant ~200 ms at 20 μM Ca^{2+}) component. These phases represent fusion of two distinct pools of primed vesicles, the rapidly releasable pool (RRP) and the slowly releasable pool (SRP). The two pools represent interconvertible states of the same docked and primed vesicles (Voets et al., 1999, and see Figure 6). The second, sustained phase of secretion, which persists for several seconds (Figures 2A and 2B), is thought to represent refilling of the primed vesicle pools, followed instantaneously by fusion as long as the $[Ca^{2+}]_i$ remains high (Voets, 2000). The amperometric signals (see Figures 2A and 2B, bottom) serve as an independent measure of secretion, based on direct detection of the released catecholamines.

In SNAP-25 mutant cells, flash-induced secretion was nearly abolished, both when evaluated as capacitance change and as amperometric current, although a small amount of slower secretion persisted (Figures 2A and 2B). We estimate that <5% of the fast secretory burst was present in mutant cells, whereas over a 5 s period, the total secretion amounted to ~13% of that seen in control cells. We therefore confirm the finding that evoked, Ca^{2+}-stimulated release is almost abolished in the absence of SNAP-25 (Washbourne et al., 2002). Anal-

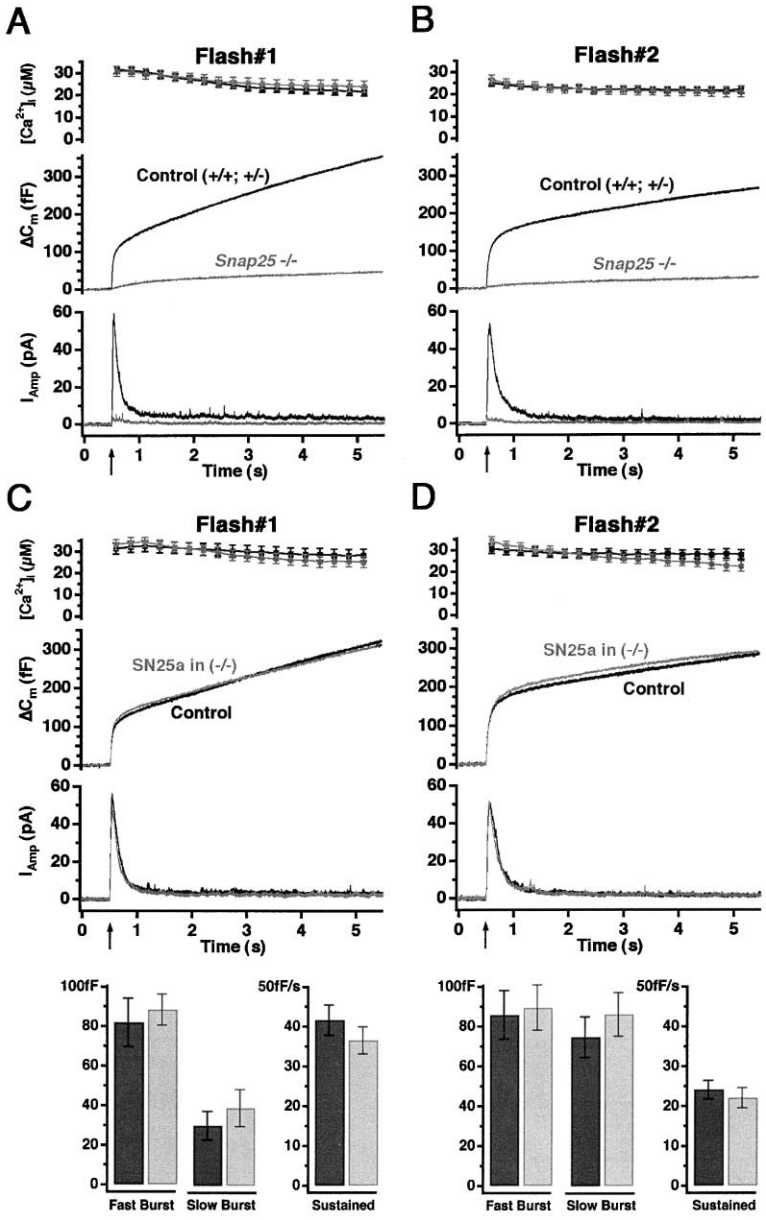

Figure 2. Fast Ca^{2+}-Triggered Secretion Is Nearly Abolished in the Absence of SNAP-25

(A–D) Flash photolysis of caged calcium increased the $[Ca^{2+}]_i$ from a basal value of 0.3–0.6 μM (data not shown) until >20 μM (top). Secretion was evaluated by simultaneous capacitance (middle) and amperometric measurements (bottom). The traces are always averages of >20 experiments; therefore, the individual fusion events (spikes) are not recognizable in the amperometric signal. The flash of UV light was given at 0.5 s (arrows). (A) Results from the first flash stimulation in control cells (*Snap25*$^{+/-}$, *Snap25*$^{+/+}$, black, n = 55 cells from 11 animals) and in SNAP-25 mutant cells (gray, n = 34 cells from five animals). Secretion in mutant cells is almost abolished. (B) Results from a second flash stimulation given ~2 min after the first one (in [A]). (C) Secretion was restored when SNAP-25 mutant cells were overexpressing SNAP-25a (gray, n = 31). The black trace is from control (n = 32) littermates. Bottom panels: the mean ± SEM of the amplitudes of the two burst components, the fast burst (corresponding to the size of the RRP) and the slow burst (corresponding to the size of the SRP). No difference was observed between control cells (black bars) and SNAP-25 mutant cells overexpressing SNAP-25a (gray bars). Likewise, the rate of the sustained component was similar. (D) Results from a second flash stimulation given ~2 min after the first one (in [C]).

ysis of data from heterozygous and homozygous wild-type animals showed no difference in the amount or kinetics of secretion (data not shown). Therefore, these data were pooled and termed control in these and future experiments.

Rescue of the Exocytotic Burst by SNAP-25 Isoforms

We next examined whether the deficiency in the Ca^{2+}-triggered exocytotic burst could be rescued by expression in mutant cells of SNAP-25a using a Semliki Forest virus (SFV) vector construct. Acutely overexpressing mutant cells (6–10 hr after transduction) were studied in parallel with cells from control littermates. As shown in Figures 2C and 2D, transduction with SNAP-25a virus rescued secretion to control levels. Further kinetic analysis was done by fitting a sum of exponential functions to the individual traces (Experimental Procedures); the amplitudes of the first two exponentials correspond to the size of the fast burst (RRP) and the slow burst (SRP) component, respectively, whereas their time constants provide information about the kinetics of release. The time constants of RRP and SRP secretion were identical between mutant cells overexpressing SNAP-25a and control cells (control: τ_1 = 21 ± 2 ms, τ_2 = 146 ± 27; SNAP-25a overexpression: τ_1 = 17 ± 1 ms, τ_2 = 169 ± 19 ms). Moreover, the size of both burst components and the rate of sustained release were indistinguishable from control cells (Figures 2C and 2D, bottom).

In the *Snap25* null mutant mouse, the expression of both SNAP-25 splice variants is disrupted (Washbourne et al., 2002). To gain insight into what physiological changes might be attributed to the developmental shift from SNAP-25a to SNAP-25b expression seen during

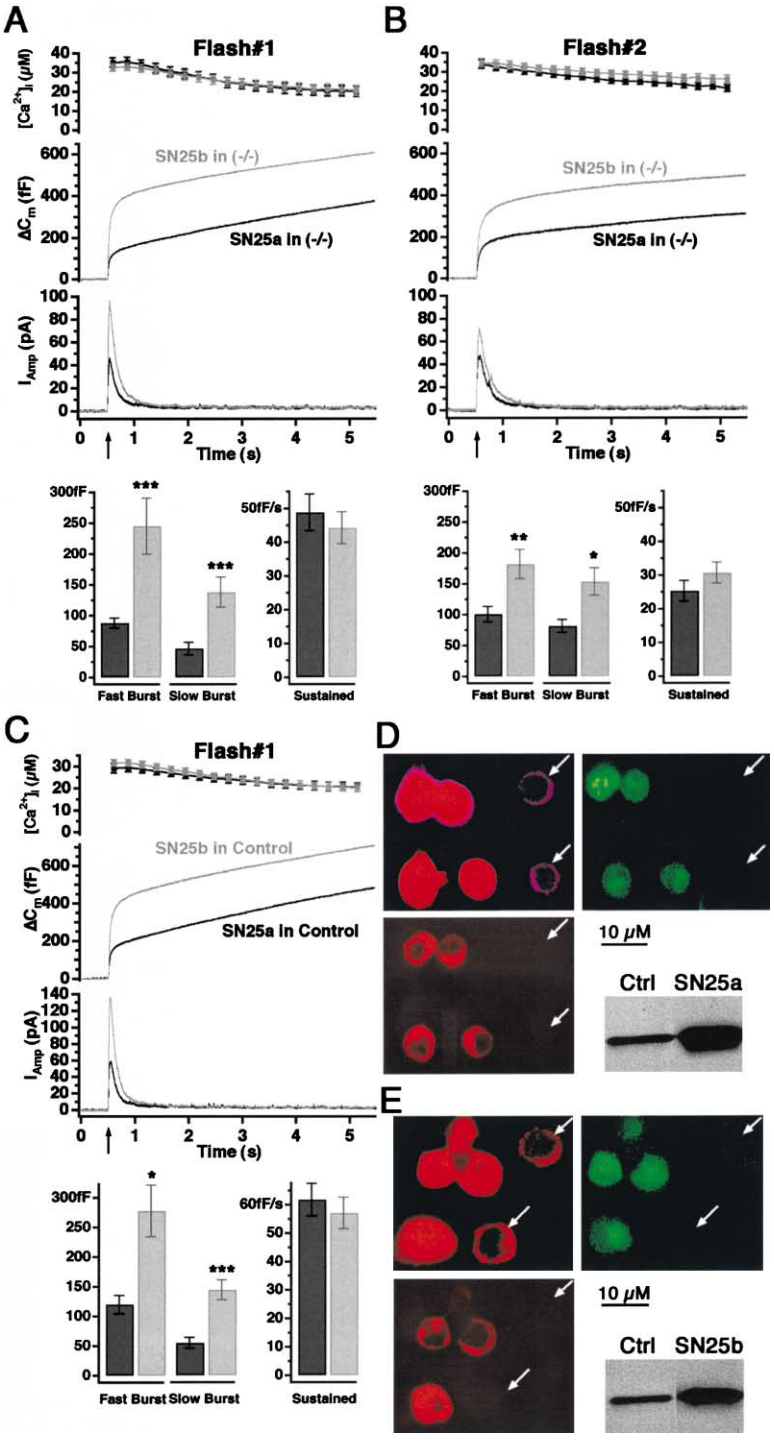

Figure 3. Differences in Releasable Vesicle Pool Sizes Induced by Splice Variants of SNAP-25

(A and B) Response to flash stimulation in SNAP-25 mutant cells overexpressing SNAP-25a (black trace, n = 29) and SNAP-25b (gray trace, n = 33). For explanation, see the legend to Figure 2. A substantial increase in secretion is seen in both capacitance and amperometric measurements when overexpressing the SNAP-25b isoform compared to SNAP-25a overexpressing cells. (B) Response to a second flash stimulation given ~2 min after the first one. Bottom panels: mean ± SEM of the amplitudes of the fast burst, the slow burst, and the rate of the sustained component (black bars, mutant cells overexpressing SNAP-25a; gray bars, mutant cells overexpressing SNAP-25b). *P < 0.05 , **P < 0.01, ***P < 0.001 (Mann-Whitney U-test).

(C) Overexpression of SNAP-25a (black trace, n = 25) and SNAP-25b (gray trace, n = 30) in control cells. For explanation, see above. Also when expressed in control cells did SNAP-25b induce a larger exocytotic burst.

(D and E) Immunocytochemistry of control embryonic mice cells overexpressing SNAP-25a (D) or SNAP-25b (E). Top right: the image taken in the green channel show which cells expressed GFP. Nonexpressing cells are marked by arrows. Top left: the first image in the red channel (specific for SNAP-25) was taken at high detector gain. The image shows the membrane distribution of SNAP-25 in the nonoverexpressing cells (arrows). Bottom left: an image taken with lower detector gain show that overexpressed protein was also present in the plasma membrane. Bottom right: Western blot with a SNAP-25 specific antibody of bovine chromaffin cells (left) and bovine cells overexpressing SNAP-25a or b.

brain development, we compared the characteristics of exocytosis after expression of either isoform in mutant cells. As seen in the previous experiments, SNAP-25a expression rescued secretion in mutant cells to control levels (compare Figure 3A and Figure 2). However, overexpression of SNAP-25b resulted in an even larger increase in secretion, effectively rescuing secretion to a level greater than SNAP-25a-expressing cells (Figure 3A). This effect was robust, as it was also present when a second flash stimulation was performed ~2 min after the first (Figure 3B). Kinetic analysis showed that the two burst components did not differ in their kinetics of fusion (SNAP-25a: $\tau_1 = 15 \pm 1$ ms, $\tau_2 = 165 \pm 24$ ms; SNAP-25b: $\tau_1 = 17 \pm 1$ ms, $\tau_2 = 128 \pm 13$ ms); however, the sizes of both the fast and the slow bursts were increased by a factor of two to three in SNAP-25b overexpressing cells (Figures 3A and 3B, bottom). In contrast, the rate of the sustained component did not vary with the isoform.

We next overexpressed SNAP-25 isoforms in control

cells. In the first series of experiments, we verified that control cells overexpressing SNAP-25a had similar secretion as noninfected control cells (see Supplemental Figure S1 online at http://www.cell.com/cgi/content/full/114/1/75/DC1), in agreement with data from bovine cells (Nagy et al., 2002). Moreover, upon overexpression of the two isoforms, SNAP-25b induced a larger exocytotic burst than SNAP-25a, which was again caused by a 2- to 3-fold increase in the size of the fast and the slow burst in the absence of a change in fusion kinetics (Figure 3C and data not shown). These data show that the effect of SNAP-25 isoforms is not limited to mutant cells and that overexpressed SNAP-25b is able to induce a higher level of secretion even in the presence of endogenous SNAP-25.

Expression and Cellular Localization of Endogenous and Viral-Expressed SNAP-25

The level of expression of the SNAP-25 isoforms provided by SFV transduction was investigated using bovine chromaffin cells because the mouse preparations do not yield enough tissue for Western blots. Using an antibody that recognizes both isoforms, we demonstrated that the viral constructs induced expression of both SNAP-25 splice variants approximately 22-fold over endogenous levels (bottom right in Figures 3D and 3E). Immunocytochemistry was used to verify expression in fetal mouse chromaffin cells from control animals. Shown in Figure 3D are fluorescence images of six chromaffin cells, four of which were expressing exogeneous SNAP-25a, as indicated by the green fluorescent protein (GFP) fluorescence (green channel). Confocal images were collected at two different detector gains to resolve the cellular localization of overexpressed and native SNAP-25 (red images; upper image, high detector gain; lower image, low detector gain), respectively. The high-gain image depicts the plasma membrane localization of endogeneous SNAP-25 in the two noninfected cells (arrows). At this high-gain setting, the signal for the four overexpressing cells was saturated. However, at lower detector gain, it was seen that a substantial proportion of the immunofluorescence in overexpressing cells was localized to the plasma membrane. At this lower gain setting, fluorescence from the noninfected cells was undetectable. Figure 3E shows the analogous result for SNAP-25b. Together, these data indicate that overexpression of either SNAP-25 isoform does not markedly alter the cellular pattern of expression.

The observed difference in secretion promoted by SNAP-25a and SNAP-25b isoforms was not due to differences in expression levels. First of all, Western blot analysis showed that the constructs expressed similar amounts of protein (above). Second, we preselected overexpressing cells for experiments based on similar fluorescence levels of the expression marker GFP (Nagy et al., 2002). Just as importantly, however, secretion in SNAP-25a overexpressing mutant or control cells was not greater than in noninfected control cells, despite considerable overexpression of the viral encoded gene, indicating that the fusion machinery is already saturated by the endogenous SNAP-25a. Thus, even if there were differences in the expression levels between SNAP-25a and SNAP-25b constructs, this could not account for the differences in secretion observed.

Overexpressed SNAP-23 Can Compete with SNAP-25, but Does Not Support an Exocytotic Burst

Adrenal chromaffin cells express low levels of SNAP-23, the widely expressed but distinct SNAP-25 homolog (Grant et al., 1999). To examine whether SNAP-23 could contribute to neuroexocytosis of LDCVs, we overexpressed it in mutant and control cells. Immunocytochemistry of both noninfected SNAP-25 mutant (Figure 4B) and control cells (Figure 4D) showed very weak staining with a SNAP-23-specific antibody (i.e., cells which do not express GFP, upper red channel figures; arrows). However, in infected cells expressing SNAP-23 and GFP, a significant proportion of the SNAP-23 appeared to accumulate at the plasma membrane (lower picture in the red channel with the detector gain reduced as described above). Western blotting using bovine chromaffin cells indicated that SNAP-23 was overexpressed $>$40-fold by the virus construct.

Overexpression of SNAP-23 in SNAP-25 mutant cells caused a small but highly significant increase in overall secretion above the low background level of these cells (Figure 4A). This increase was due to a somewhat steeper sustained component of release, whereas an exocytotic burst was still absent. Conversely, when overexpressed in control cells, SNAP-23 caused a significant decrease in overall secretion (Figure 4C). Comparing mutant and control cells overexpressing SNAP-23, it was apparent that secretion converged to the same level in the presence of an excess of SNAP-23; however, in control cells a residual small exocytotic burst was seen, probably because some SNAP-25 still participates in secretion. These data show that SNAP-23 can indeed participate in secretion and substitute for SNAP-25; however, the secretion displays different features from SNAP-25-induced secretion, especially the absence of an exocytotic burst.

Stimulation by Ca^{2+} Infusion

Based on the studies above, it is clear that in the absence of SNAP-25 the Ca^{2+}-triggered exocytotic burst from chromaffin cells is greatly diminished, leaving only a small amount of sustained secretion. To study the remaining secretion in greater detail, we again took advantage of the coupled patch clamp/amperometric system. In these experiments, cells were perfused with Ca^{2+}-containing solutions via the patch pipette while assaying secretion using a carbon fiber placed in direct contact with the cell. We preferred amperometric detection in these extended experiments because capacitance measurements would be contaminated with slow endocytotic processes.

As shown in Figure 5A, infusion with $\sim$10 μM Ca^{2+} resulted in robust secretion from control cells. Moreover, mutant cells also responded with distinct amperometric spikes, albeit at significantly lower frequencies. To evaluate whether the secretion was calcium dependent, we also perfused cells with lower $[Ca^{2+}]_i$ ($<$1 μM) and counted amperometric spikes to calculate the release frequency during the first minute of release. In the low-Ca^{2+} solution, the release frequencies of mutant and control cells were indistinguishable (Figure 5B). In the presence of high $[Ca^{2+}]_i$, the frequency of release

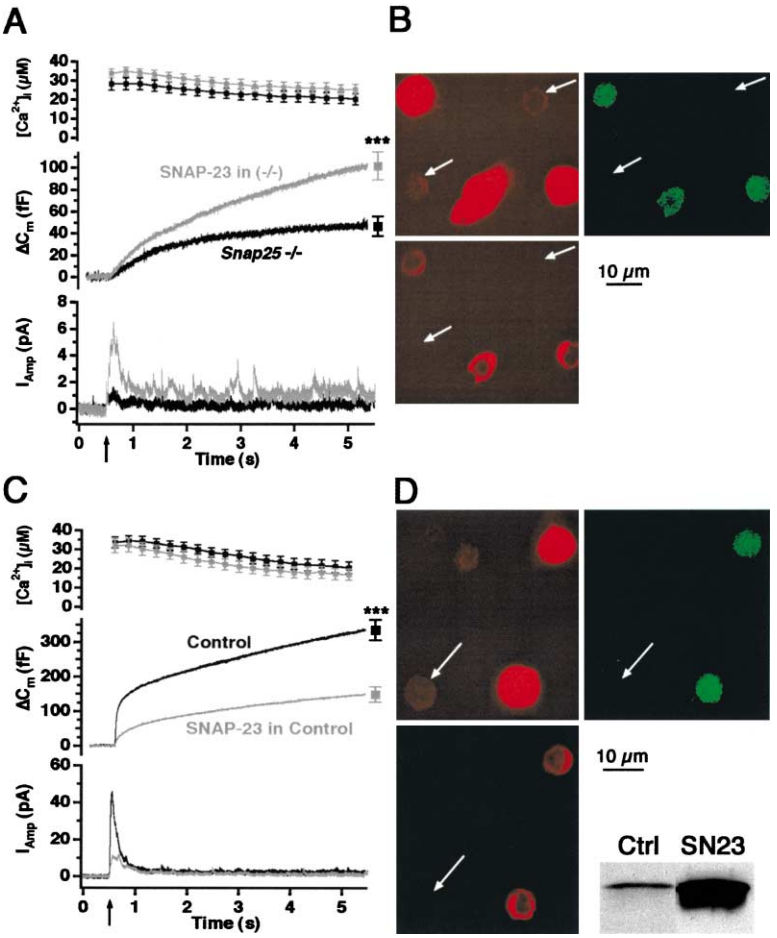

Figure 4. SNAP-23 Competes with SNAP-25 for Participation in Secretion

(A) Response to flash stimulation in SNAP-25 mutant cells (black, n = 23), and in mutant cells overexpressing SNAP-23 (gray, n = 27). Overexpression of SNAP-23 increased the total secretion seen during 5 s. after the flash (squares with error bars: mean ± SEM of total secretion).

(B) Immunocytochemistry of SNAP-25 mutant cells overexpressing SNAP-23. Top right: GFP fluorescence, Top and bottom left: SNAP-23 specific channel with high (top) and low (bottom) detector gain. See also legend to Figures 3D and 3E. The data show the partial plasma membrane localization of overexpressed SNAP-23. Native SNAP-23 was weakly expressed.

(C) Response to flash stimulation in control cells (black, n = 22) and in control cells overexpressing SNAP-23 (gray, n = 21). A significant decrease in the total secretion occurred upon overexpression of SNAP-23.

(D) Immunocytochemistry of control embryonic mice cells overexpressing SNAP-23 confirms the plasma membrane localization for SNAP-23. Explanations as for (B). Bottom right: Western blot with a SNAP-23 specific antibody of bovine chromaffin cells (left) and bovine cells overexpressing SNAP-23 (right). ***P < 0.001 (Mann-Whitney U-test).

increased in both cell types; however, the increase was significantly larger in control cells. Nevertheless, the mutant cells still reached a release frequency around one-third of that in control cells, indicating that release is still Ca^{2+} dependent in the absence of SNAP-25. This conclusion was supported from data in some mutant cells perfused with the low-Ca^{2+} solution, where the $[Ca^{2+}]_i$ happened to increase suddenly either because of a leaky seal or because the cells were intentionally depolarized. In these cells, the release frequency increased shortly after the increase in $[Ca^{2+}]_i$ (Figure 5C).

The amperometric measurements provide information about the kinetics of catecholamine release from individual vesicles, starting at the time a fusion pore forms that is large enough to allow escape of catecholamines. We therefore identified individual spikes and estimated spike charge (Q), peak amplitude, halfwidth (i.e., duration at half amplitude), 50%–90% risetime, and the duration of the so-called foot signal (Figures 5D and 5E). The foot signal is believed to reflect the initial formation of a permeable fusion pore (Chow et al., 1992), whereas the subsequent spike represents the dilation of the fusion pore and emptying of vesicular contents during full fusion. We determined the cumulative distribution of each spike parameter in each cell analyzed and calculated a weighted overall cumulative distribution, where each cell is included with the same weight regardless of the number of spikes recorded. The distributions showed no noticeable differences between mutant and control cells for the charge (Figure 5F), peak amplitude (Figure 5G), risetime (Figure 5H), and halfwidth (Figure 5I), indicating that the spikes in mutant cells were normal in overall appearance. However, surprisingly the distribution of the foot duration indicated a significantly shorter foot duration in the mutant cells (Figure 5J, Table 1). Consequently, we next tested whether overexpression of SNAP-25a, SNAP-25b, or SNAP-23 in mutant cells changed the appearance of the single amperometric spikes. We again found no significant differences upon overexpression, except that the normal foot duration was rescued in all three experiments (Table 1).

Discussion

SNAP-25 and Vesicle Docking

Studies in several organisms have shown that SNARE complex assembly is not involved in the initial membrane attachment of secretory vesicles (reviewed by Jahn and Südhof, 1999). In the present study, we extend these findings by showing that morphological docking of LDCVs in chromaffin cells appears intact in the absence of SNAP-25 (Figure 1). In contrast, similar analysis in *munc18-1* null mutant mice demonstrated that the docking of LDCVs was blocked (Voets et al., 2001b). Other studies have implicated that SNAP-25 may act through calcium-dependent binding of synaptotagmin I

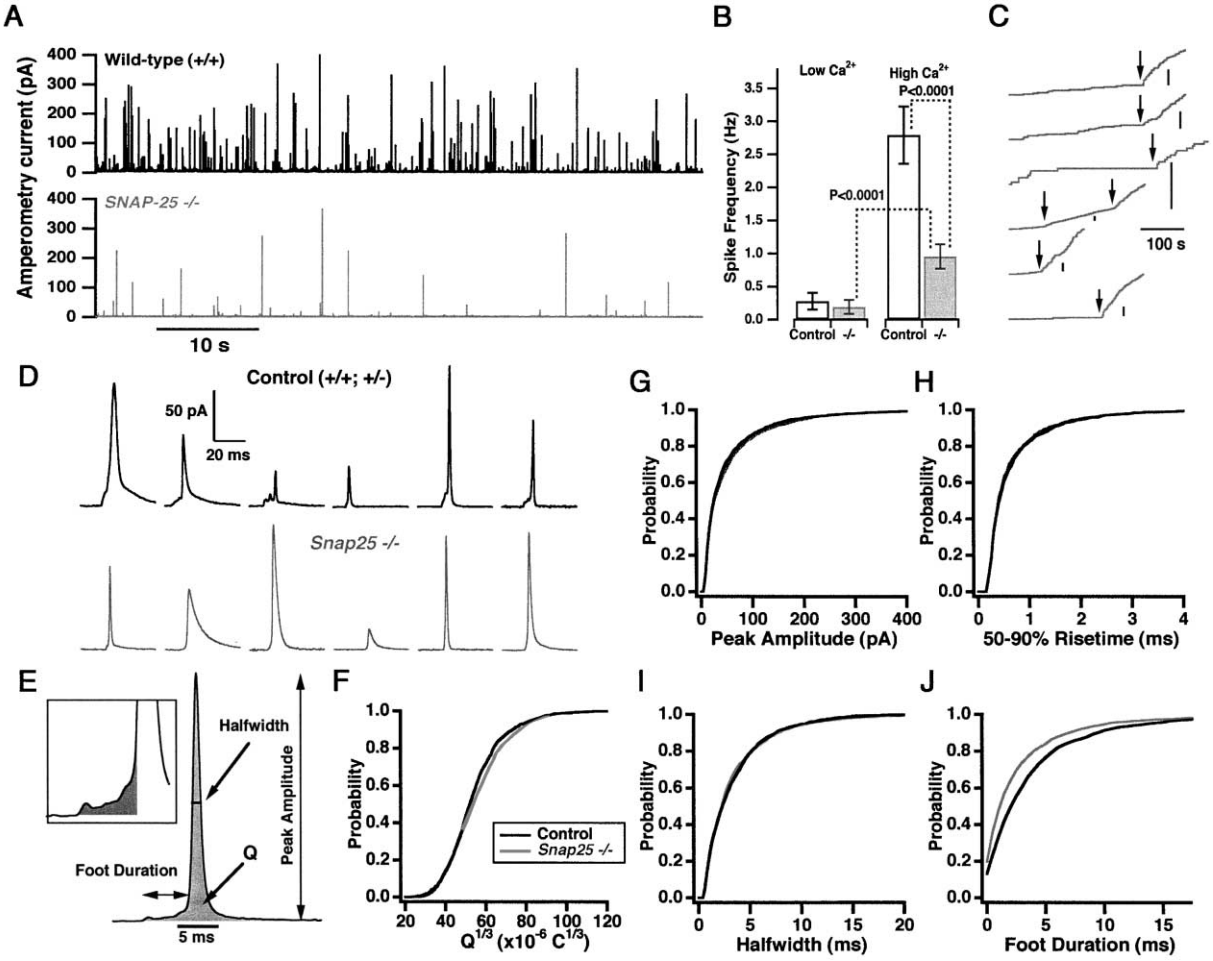

Figure 5. Secretion in the Absence of SNAP-25 Is Stimulated by Ca^{2+} Infusion

(A) Amperometric current from example wild-type cell (*top*, black trace) and SNAP-25 mutant cell (*bottom,* gray trace) infused with ~10 μM calcium through the patch pipette. Each spike represents the fusion of one vesicle.

(B) Release rates (Mean ± SEM) for control (black bars) and SNAP-25 mutant cells (gray bars) perfused with low-Ca^{2+} solution (<1 μM, left two bars) or high-Ca^{2+} solution (10 μM, right two bars). At low Ca^{2+}, both cell types displayed similar release rates, and at high Ca^{2+}, the control cells had significantly higher rates.

(C) Integration of the number of fused vesicles (vertical bars represent 20 spikes, note that each experiment has its own vertical calibration bar) as a function of time in six SNAP-25 mutant cells, where the $[Ca^{2+}]_i$ increased abruptly during measurements (at arrows). $[Ca^{2+}]_i$ was measured during the experiment by inclusion of calcium-sensitive dyes in the pipette solutions. Note that in every case did the rate of release increase shortly after the increase in $[Ca^{2+}]$, indicating that secretion from mutant cells was Ca^{2+} dependent.

(D) Examples of different spike shapes in control cells (black) and SNAP-25 mutant cells (gray). The spikes were chosen in order to illustrate the diversity in spike form in both cell types.

(E) Analysis of a single amperometric spike. Shown is the estimation of peak amplitude, halfwidth, foot duration, and charge (Q). Inset shows the foot in higher resolution. The area identified as the foot is shown in gray.

(F–J) Normalized cumulative distributions of the cubic-root of the charge (F), the peak amplitude (G), the 50%–90% risetime (H), the halfwidth (I), and the foot duration (J). In these distributions each cell recorded enters with the same weight. Black traces: control cells, gray traces: SNAP-25 mutant cells. The data show that the foot duration is shorter in SNAP-25 mutant cells, whereas all other parameters are unchanged.

to promote vesicular docking (Chieregatti et al., 2002). However, docking proceeds normally in hippocampal neurons of *synaptotagmin I* null mutant mice (Geppert et al., 1994), suggesting that synaptotagmin I is not essential for this process. Also, our data on SNAP-25 mutants argue against an essential role for an interaction between synaptotagmin I and SNAP-25 in vesicle docking. However, this does not rule out a role for the potential interplay between these proteins downstream from docking, as suggested by Zhang et al., 2002 (but see Shin et al., 2003 for a different view).

Secretion in the Absence of SNAP-25

After stimulation by flash photolysis of caged Ca^{2+}, SNAP-25 mutant chromaffin cells displayed a complete absence of fast, synchronized release (Figure 2). In principle, this could be due either to a direct effect of the loss of SNAP-25 expression or to a secondary effect due to differences in ontogeny. Therefore, as a prelude to this project, we developed a preparation of isolated chromaffin cells from single embryonic mice (Experimental Procedures), which allowed cells to be kept in primary culture and infected with viral constructs car-

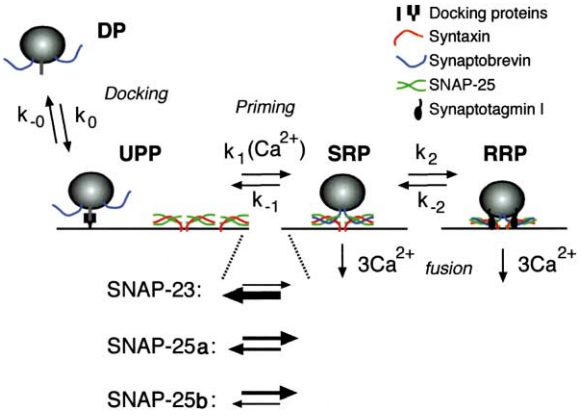

Figure 6. Kinetic Model of Vesicle Docking, Priming, and Fusion

A linear model of vesicle maturation including docking, priming, and fusion (Voets, 2000; Ashery et al., 2000). Abbreviations: DP, depot pool; UPP, pool of docked but unprimed vesicles; SRP, slowly releasable pool; and RRP, rapidly releasable pool. The docking is attributed to a set of docking proteins. The priming step corresponds to the assembly of the SNARE complex (shown simplified), and the further maturation into the RRP requires synaptotagmin I (Voets et al., 2001a). Fusion from the SRP and RRP is assumed to require three Ca^{2+} ions. For simplicity, synaptotagmin I and the docking proteins are only shown in the stages where they play a role. The relative rates of priming and depriming for SNAP-23, SNAP-25a, and SNAP-25b are symbolized by the thickness of the arrows.

rying SNAP-25. Our data on control littermates (Figures 2A–2D) show that the release competence of these isolated cells is not different from that of mouse adrenal slices (Voets et al., 1999; Voets, 2000). Complementation by acute overexpression of SNAP-25a (Figures 2C and 2D) demonstrated, importantly, that except for the lack of SNAP-25 the release machinery is intact in mutant cells.

Although fast Ca^{2+}-triggered secretion was almost abolished, SNAP-25 mutant cells could be stimulated to secrete at one-third the rate of controls when perfused with a Ca^{2+}-containing solution (Figure 5). Thus, fast Ca^{2+}-triggered release is affected more by the lack of SNAP-25 than is the single spike rate in infusion experiments. This result is reminiscent of the differences observed in neurons between evoked release and action potential-independent spontaneous release (a minimal synaptic response known as a "mini") when a SNARE component was deleted. Thus, a high frequency of minis could be recorded at the neuromuscular junction of these SNAP-25-deficient mutant mice, although evoked release was absent (Washbourne et al., 2002). Similar observations have been made when synaptobrevin was deleted (Deitcher et al., 1998; Schoch et al., 2001). These findings show that the neuronal SNARE complex is not absolutely required for fusion, prompting the speculation that vesicles may fuse either without SNAREs (Schoch et al., 2001) or by the help of an alternative SNARE complex (Scales et al., 2001; Washbourne et al., 2002).

The single spike analysis showed that single fusion events were largely normal in the absence of SNAP-25 (Figure 6, Table 1). This indicates that once the fusion pore expands, fusion proceeds normally in the absence of SNAP-25. This is an important finding since previous reports showed that overexpression of C-terminal SNAP-25 mutants resulted in spikes with slower kinetics (Gil et al., 2002). Upon closer analysis, we found that the duration of the foot signal was significantly shorter in SNAP-25 mutant cells. A shorter foot signal means that the lifetime of the fusion pore is shorter in the absence of SNAP-25, with fusion pores expanding faster into full fusion events. Thus, whereas the SNARE complex obviously increases the probability of vesicle fusion, it also may counteract the expansion of the pore once the fusion pore is formed. It is important to note that the SNARE complex will be transformed from a *trans* complex into a *cis* complex, if formation of the fusion pore implies fusion of the lipid membranes. The strong tendency of the complex to zipper up, which may originally have driven lipid mixing (Hanson et al., 1997), will now be unable to apply force to the membranes. In this situation, it is conceivable that the presence of *cis* complexes may interfere with the expansion of the fusion pore. An alternative explanation may be that another protein/protein complex that is bound to the SNARE complex may interfere with fusion pore expansion. Indeed, synaptotagmin I overexpression causes a longer duration of the fusion pore (Wang et al., 2001).

Considering these potential explanations raises several possibilities for the role of SNAREs in the sustained level of secretion seen in the *Snap25* null mutant mouse. In the absence of SNAP-25 or other neural SNARE com-

Table 1. Single Fusion Event Characteristics as Measured by Amperometry

			Cell Medians				
	Number of Cells	Number of Spikes	Amplitude (pA)	$Q^{1/3}$ ($\times 10^{-6}$ $C^{1/3}$)	Halfwidth (ms)	Risetime (ms)	Foot Duration (ms)
Control	28	2419	34 ± 3	53 ± 1	2.8 ± 0.3	0.48 ± 0.03	2.7 ± 0.2
SNAP-25 −/−	43	3271	35 ± 2	54 ± 1	2.5 ± 0.2	0.46 ± 0.02	1.7 ± 0.1**
SNAP-25a in −/−	15	1407	38 ± 3	59 ± 2	3.0 ± 0.5	0.44 ± 0.03	2.5 ± 0.2
SNAP-25b in −/−	14	1062	43 ± 5	56 ± 3	2.4 ± 0.4	0.43 ± 0.05	2.7 ± 0.4
SNAP-23 in −/−	15	1403	40 ± 5	59 ± 3	2.8 ± 0.5	0.49 ± 0.05	3.3 ± 0.4

In columns two and three is shown the number of cells and spikes analyzed for each condition. The table gives mean ± SEM of the cell median of each parameter, thus the n that enters into the calculation of the SEM (and the statistical tests) is the number of cells, not the number of spikes. Except for the foot duration, all other comparisons were nonsignificant.** In a one-way analysis of variance the difference between cell populations was very significant ($p < 0.0001$) and posttest showed that the SNAP-25 mutant cells were significantly different from control cells ($p < 0.01$)

ponents (e.g., synaptobrevin; Schoch et al. 2001), vesicles may fuse either without the assistance of a SNARE complex or an alternative SNARE complex is present, although the nature of this SNARE complex is unknown. Because SNAP-23 is the most likely alternative to SNAP-25 and overexpression of both SNAP-23 and SNAP-25 rescued the fusion pore duration (Table 1), this may suggest that vesicles in the SNAP-25 mutant fused without the assistance of either isoform. Alternatively, the significant overexpression of SNAP-23 provided by SFV vector expression may rescue the foot signal through mass action. Such a model would be consistent with the idea that in the SNAP-25 mutant, fewer (presumably SNAP-23 containing) SNARE complexes may be involved in each fusion event, so that the proposed action of SNAREs to initially restrict expansion of the fusion pore would be impaired leading to loss of the foot. That SNAP-23 appears to be low in abundance in chromaffin cells is consistent with both of these models.

Secretion in the Presence of SNAP-25 Splice Variants and SNAP-23

A question of considerable current interest is to which degree is SNARE interaction specific? The SNARE hypothesis stated that recognition between specific v-SNAREs and t-SNAREs form the basis for specificity in vesicle targeting (Söllner et al., 1993). Efforts to test this hypothesis have been met with differing results and interpretations (reviewed by Rizo and Südhof, 2002). A question that has received less attention is what is the role of different cognate SNARE complexes? In the exocytotic pathway of neurosecretory cells, both SNAP-25 and SNAP-23 may be present (Grant et al., 1999), and both can form SNARE complexes including the v-SNARE synaptobrevin 2. Whereas syntaxin 1 is the cognate t-SNARE partner of SNAP-25 (Söllner et al., 1993), SNAP-23 can bind syntaxin 1, 2, 3, and 4 (Ravichandran et al., 1996). The alternative splicing of SNAP-25 (Bark and Wilson, 1994) gives rise to yet another level of complexity.

Using acute overexpression in SNAP-25 mutant cells, we provide evidence that at least three different functional SNARE complexes can play a part in driving the same exocytotic event, although the characteristics of secretion promoted by the isoforms are different. A linear model of vesicle maturation (Figure 6) was previously shown to account for data obtained from chromaffin cells (Voets et al., 1999; Ashery et al., 2000; Voets, 2000). This model contains two forms of releasable vesicles, represented by two pools—the readily releasable pool (RRP) and the slowly releasable pool (SRP)—which were shown to be arranged sequentially (Voets et al., 1999). Our current results show that SNAP-25b-driven secretion is characterized by a more than 2-fold larger size of the SRP and the RRP, whereas the sustained component and the kinetics of fusion of the two releasable pools are unchanged compared to SNAP-25a (Figure 3). Since the size of both releasable pools change in parallel, this means that the isoform specificity affects the step upstream of maturation of vesicles into the SRP, i.e., the priming step. However, in the model, the sustained component of release is caused by rapid priming followed by fusion at the high $[Ca^{2+}]_i$ following the flash (the rate constant k_1 is calcium dependent; Voets et al., 1999). Since the sustained component is not affected, the isoform specificity of SNAP-25 must act during depriming, i.e., the rate constant k_{-1} (Figure 6) is reduced in the presence of SNAP-25b, whereas the priming rate (k_1) is unaffected by SNAP-25 isoform. SNAP-23-driven secretion was characterized by a sustained release rate intermediate between mutant cells and SNAP-25-overexpressing cells (Figure 4). This suggests the priming rate (k_1) ranking as SNAP-23 $<$ SNAP-25a $=$ SNAP-25b (Figure 6). A further characteristic of SNAP-23 driven secretion was the absence of a standing pool of primed vesicles. This suggests that primed vesicles that do not fuse are rapidly lost again by depriming, preventing the build-up of a primed pool. Taken together with the results obtained for the SNAP-25a/b isoforms, we suggest that these constituents of the SNARE complex vary in their ability to stabilize vesicles in the releasable vesicle pools, ranking the relative priming stability as SNAP-25b $>$ SNAP-25a $>>$ SNAP-23 or, equivalently, that the depriming rate (k_{-1}) ranks as SNAP-23 $>>$ SNAP-25a $>$ SNAP-25b (Figure 6).

It must be stressed that for technical reasons we have not been able to measure the depriming rate directly. Originally, reversibility of the priming process was postulated in the model to limit the size of the releasable pools, SRP and RRP (Voets et al., 1999). In addition, vesicle depriming was observed in chromaffin cells (Smith et al., 1998). However, another way of limiting the size of the releasable vesicle pools would be to postulate that SNAP-25 (maybe together with syntaxin 1) would form a part of a priming site, which would be in limited supply. This would introduce an upper limit for the number of release-ready vesicles. In that model, the effect of SNAP-25 isoform would be on this upper limit, whereas the rate of depriming would not have to be modified. Furthermore it should be noted that in the model (Figure 6), the priming step is lumped into one reaction, whereas in reality, priming probably involves several consecutive reactions.

Our finding that SNAP-25a overexpression rescued secretion to control levels is consistent with previous evidence showing that SNAP-25a mRNA is the prevalent transcript in adrenal medulla (Bark et al., 1995; Grant et al., 1999) but importantly adds that the SNAP-25a isoform is the major functional isoform. The difference in the size of the releasable pools attributed by the incorporation of either SNAP-25a or SNAP-25b isoforms into the neuronal SNARE complex suggests that the progressive increase in SNAP-25b mRNA relative to SNAP-25a during the first weeks of postnatal brain development (Bark et al., 1995) could be required for increasing pools of primed vesicles to meet the needs of synaptic maturation. Furthermore, since a primed pool of vesicles is essential for fast Ca^{2+}-triggered exocytosis, it may be necessary for neurosecretory cells and neurons to ensure that SNAP-25, not SNAP-23, will participate in vesicle priming. Thus, our overexpression studies show that if present in the same cell, exogeneous SNAP-23 and SNAP-25b can compete with endogeneous SNAP-25a; whether this is of significance in vivo or whether cells regulate expression to assure that only one SNARE component is functional remains to be seen.

Our data raise interesting questions about the under-

lying biochemical properties responsible for the differences in vesicle pool sizes observed between the two SNAP-25 isoforms and SNAP-23. One possibility is that the three SNARE complexes display different intrinsic tendencies to dissociate under stress, i.e., when they link the membranes together in *trans*, which may result in different rates of spontaneous depriming of vesicles. Indeed, SNARE core complexes including SNAP-23 are not SDS resistant and appear less thermostable (Yang et al., 1999). Another possibility is that the vesicle pool size is a regulated feature contributed by auxiliary factors binding to the outside of the SNARE complex. SNAP-25, but not SNAP-23, may interact with such factors and thereby confer stability to the fusion machinery. Future experiments will be needed to distinguish between these possibilities.

Regardless of the precise mechanism for setting the sizes of the releasable vesicle pools, our findings support the idea that the neuronal variety of the SNARE complex simultaneously increases the priming rate and decreases the depriming rate. The net result of these two effects is to trap vesicles in the pool of primed vesicles. The formation of this standing pool of primed vesicles is a condicio sine qua non for fast Ca^{2+}-triggered exocytosis, defining a population of vesicles on which the fast calcium trigger—presumably mediated by one or more synaptotagmin isoforms—can act during the brief duration of an evoked calcium signal.

Experimental Procedures

Preparation of Embryonic Mouse Chromaffin Cells

Following caesarean section, embryonic adrenal glands were dissected, placed in filtered Locke's solution (154 mM NaCl, 5.6 mM KCl, 0.85 mM NaH_2PO_4, 2.15 mM Na_2HPO_4, and 10 mM Glucose [pH 7.0]), and cleaned free of connective tissue. The glands were incubated with 0.2 ml papain solution (see below) at 37°C for 40 min with slight shaking, followed by addition of 150 μl inactivating solution for 5 min. The solution was then carefully replaced by 0.2 ml enriched DMEM medium and the glands triturated gently through a 200 μl pipette tip. 50 μl of the cell suspension was plated on each sterile coverslip in 6-well plates, the cells were allowed to settle before supplementing with enriched medium. The cells were incubated at 37°C and 10% CO_2 and used within 3 days. Papain solution: 250 ml DMEM medium (Linaris, Wertheim-Bettingen, Germany) supplemented with 50 mg L-Cysteine, 2.5 ml 0.1 M $CaCl_2$, 2.5 ml 50 mM EDTA, and 20–25 units/ml papain (Worthington, Lakewood, NJ) and equilibrated with 5% CO_2. Inactivating solution: 225 ml DMEM medium supplemented with 25 ml heat inactivated fetal calf serum (Invitrogen, San Diego, CA), 625 mg albumin, 625 mg trypsin inhibitor (Sigma, St. Louis, MO). Enriched DMEM medium: 500 ml DMEM supplemented with 2 ml penicillin/streptomycin (Invitrogen) and 5 ml insulin-transferrin-selenium-X (Invitrogen).

Ultrastructural Analysis

Isolated chromaffin cells were fixed with 2.5% glutaraldehyde in 0.1 M phosphate buffer (for 1 hr at 4°C), osmicated with 1% osmium tetroxide in phosphate buffer (for 1 hr at 4°C), dehydrated with ethanol followed by propylene oxide, embedded in Durcupan (Fluka, Buchs, Switzerland), and polymerized (48 hr, 60°C). 50 nm "light-gold" ultrathin sections were contrasted and observed in a LEO 912AB TEM. Digital images were acquired at a magnification of 100,800× with a GrabBit Proscan CCD camera and analyzed with the Esivision software (Soft-Imaging System, Münster, Germany).

Electrophysiological Recordings

Whole-cell patch-clamp, capacitance, and calcium measurements as well as flash photolysis of caged Ca^{2+} was performed as previously described (Nagy et al., 2002). Nitrophenyl-EGTA was supplied by G. Ellis-Davies (MCP Hahnemann University, Philadelphia, PA). Intracellular calcium concentrations were measured with two dyes as described (Voets, 2000; Sørensen et al., 2002). For kinetical analysis individual capacitance traces were fitted with a triple exponential function:

$$f(t) = A_0 + \sum_{i=1}^{3} A_i \cdot (1 - \exp(-(t - t_0)/\tau_i)) \qquad \text{for } t > t_0,$$

where A_0 is the capacitance of the cell before the flash and t_0 is the time of the flash. The amplitudes (A_i) and time constants (τ_i) of the two faster exponentials define the size and release kinetics of the fast and the slow exocytotic burst, respectively. The third exponential corrected for the sustained component but was not used directly. Instead, we subtracted the size of the fast and slow burst from the total amount of secretion during 5 s and calculated the average rate of sustained release.

Amperometry

Amperometric fibers were prepared as described (Schulte and Chow, 1996). Carbon fibers were 10 μm in diameter (P-100S; Amoco Corp., Greenville, SC). Fibers were clamped to +720mV and the tip of the fiber was pressed gently against the cell. Currents were amplified and filtered at 3 kHz by an EPC-7 (HEKA Elektronik, Lambrecht/Pfalz, Germany). Upon loading into Igor Pro version 3.16PPC (Wavemetrics, Lake Oswego, OR) currents were digitally filtered at 600 Hz (Gaussian filter) and subjected to analysis by a macro. For single spike analysis, spikes larger than 10 pA were considered. When calculating release rates, spikes larger than 4 pA were included.

Two problems hamper the analysis of single amperometric spikes: overlapping spikes and cell-to-cell variability. The first problem is caused by the fact that overlapping spikes cannot be analyzed. When analyzing two different cell populations with very different release rates, this can lead to sampling error, because in the cell type with the higher release rate, slower spikes will have a higher probability of overlapping with another spike than a fast spike; thus, slower spikes will become underrepresented in the analysis. We circumvented this problem by imposing an artificial dead time, set to 50 ms, so that only those spikes were considered where the peak of another spike did not appear within a time interval 50 ms before and after the spike in question. Since 50 ms was long enough that a spike reaching the peak outside of this interval would not prevent the analysis of the spike in question, this procedure eliminated slow and fast spikes with the same probability.

The other problem is caused by the large number of events per cells combined with a large cell-to-cell variability in spike parameters, which can cause errors if the spikes are pooled for statistical testing (Colliver et al., 2000). We therefore used all spikes recorded in a cell to estimate one statistic per cell (the cell median of each spike parameter) and compared this statistic between cell populations (Table 1). Only cells where at least ten spikes were recorded entered the analysis. The maximum number of spikes analyzed per cell was set to 130.

Preparation of Viral Constructs

A modified pSFV1 (Invitrogen) plasmid was used, where an internal ribosome entry site from polio virus had been inserted followed by the gene for enhanced GFP, as described (Sørensen et al., 2002). A plasmid containing full-length mouse *Snap23/syndet* was kindly provided by Giulia Baldini (Department of Anatomy and Cell Biology, Columbia University, New York, NY; Koticha et al., 1999). The genes coding for SNAP-25a, SNAP-25b, and SNAP-23 were amplified by PCR and inserted upstream of the internal ribosome entry site using BamHI and BssHII restriction sites. All constructs were verified by DNA sequencing.

Immunoblotting and Immunocytochemistry

Bovine chromaffin cell preparation and Western Blot procedure were performed as described (Nagy et al., 2002). The primary antibodies used were mouse anti-SNAP-25 (1:10,000, Cl 71.2), and rabbit anti-SNAP-23 antiserum (1:10,000); both were a kind gift from Reinhard Jahn (Max-Planck-Institute for Biophysical Chemistry, Göttingen, Germany). The expression level of virus infected chro-

maffin cells was determined by blotting a dilution sequence of cell lysates from control and overexpressing cells, and quantifying the ECL signals in the linear range by NIH Image version 1.62 (NIH, USA). The results were corrected for the infection efficiency, which was estimated by the ratio of GFP expressing cells to the total cell number.

For immunocytochemistry, chromaffin cells were fixed in 3.7% formaldehyde in PBS for 15–20 min, washed three times with PBS, permeabilized, and blocked by 0.2% Triton X-100 and 2% normal goat serum in PBS for 1 hr, and incubated overnight at 4°C with the primary antibody diluted in blocking solution (mouse anti-SNAP25 and rabbit anti-SNAP-23, 1:2000). Following washing, the cells were incubated with secondary antibody (Alexa546-conjugated goat anti-mouse [Molecular Probes, Eugene, OR] and Cy3-conjugated goat anti-rabbit IgG [Jackson ImmunoResearch, Wester Grove, PA], 1:1000, respectively) for 1 hr at room temperature, washed again, and were finally mounted. The fluorescence was analyzed on a Zeiss LSM 410 laser scanning microscope. Optical sections of 1 μm were obtained and processed by LSM Version 3.98 software (Zeiss, Oberkochen, Germany).

Acknowledgments

We thank Reinhard Jahn and Dirk Fasshauer for commenting on the manuscript. We also thank Ina Herfort and Dirk Reuter for expert technical assistance. This work was supported by an NIH grant (NIH MH48989 to M.C.W.), a grant from the Deutsche Forschungsgemeinschaft (SFB 523 to E.N.), and an INTAS grant (No. 01-2095 to E.N.). G.N. is a Ph.D. student of the International MD/PhD Program in the Neurosciences of the International Max Planck Research School and holds a fellowship by the Deutsche Forschungsgemeinschaft (Graduiertenkolleg 521).

Received: April 3, 2003
Revised: May 19, 2003
Accepted: May 30, 2003
Published: July 10, 2003

References

Ashery, U., Varoqueaux, F., Voets, T., Betz, A., Thakur, P., Koch, H., Neher, E., Brose, N., and Rettig, J. (2000). Munc13-1 acts as a priming factor for large dense-core vesicles in bovine chromaffin cells. EMBO J. *19*, 3586–3596.

Bark, I.C., and Wilson, M.C. (1994). Human cDNA clones encoding two different isoforms of the nerve terminal protein SNAP-25. Gene *139*, 291–292.

Bark, I.C., Hahn, K.M., Ryabinin, A.E., and Wilson, M.C. (1995). Differential expression of SNAP-25 protein isoforms during divergent vesicle fusion events of neural development. Proc. Natl. Acad. Sci. USA *92*, 1510–1514.

Chen, Y.A., and Scheller, R.H. (2001). SNARE-mediated membrane fusion. Nat. Rev. Mol. Cell Biol. *2*, 98–106.

Chieregatti, E., Witkin, J.W., and Baldini, G. (2002). SNAP-25 and synaptotagmin 1 function in Ca^{2+}-dependent reversible docking of granules to the plasma membrane. Traffic *3*, 496–511.

Chow, R.H., von Lüden, L., and Neher, E. (1992). Delay in vesicle fusion revealed by electrochemical monitoring of single secretory events in adrenal chromaffin cells. Nature *356*, 60–63.

Colliver, T.L., Hess, E.J., Pothos, E.N., Sulzer, D., and Ewing, A.G. (2000). Quantitative and statistical analysis of the shape of amperometric spikes recorded from two populations of cells. J. Neurochem. *74*, 1086–1097.

Deitcher, D.L., Ueda, A., Stewart, B.A., Burgess, R.W., Kidokoro, Y., and Schwarz, T.L. (1998). Distinct requirements for evoked and spontaneous release of neurotransmitter are revealed by mutations in the Drosophila gene neuronal-synaptobrevin. J. Neurosci. *18*, 2028–2039.

Dodge, F.A., and Rahamimoff, R. (1967). Co-operative action of calcium ions in transmitter release at the neuromuscular junction. J. Physiol. (Lond.) *193*, 419–432.

Geppert, M., Goda, Y., Hammer, R.E., Li, C., Rosahl, T.W., Stevens, C.F., and Südhof, T.C. (1994). Synaptotagmin I: a major Ca^{2+} sensor for transmitter release at a central synapse. Cell *79*, 717–727.

Gil, A., Gutierrez, L.M., Carrasco-Serrano, C., Alonso, M.T., Viniegra, S., and Criado, M. (2002). Modifications in the C terminus of the synaptosome-associated protein of 25 kDa (SNAP-25) and in the complementary region of synaptobrevin affect the final steps of exocytosis. J. Biol. Chem. *277*, 9904–9910.

Gonelle-Gispert, C., Halban, P.A., Niemann, H., Palmer, M., Catsicas, S., and Sadoul, K. (1999). SNAP-25a and -25b isoforms are both expressed in insulin-secreting cells and can function in insulin secretion. Biochem. J. *339*, 159–165.

Grant, N.J., Hepp, R., Krause, W., Aunis, D., Oehme, P., and Langley, K. (1999). Differential expression of SNAP-25 isoforms and SNAP-23 in the adrenal gland. J. Neurochem. *72*, 363–372.

Hanson, P.I., Roth, R., Morisaki, H., Jahn, R., and Heuser, J.E. (1997). Structure and conformational changes in NSF and its membrane receptor complexes visualized by quick-freeze/deep-etch electron microscopy. Cell *90*, 523–535.

Hepp, R., Dupont, J.L., Aunis, D., Langley, K., and Grant, N.J. (2001). NGF enhances depolarization effects on SNAP-25 expression: induction of SNAP-25b isoform. Neuroreport *12*, 673–677.

Jahn, R., and Südhof, T.C. (1999). Membrane fusion and exocytosis. Annu. Rev. Biochem. *68*, 863–911.

Koticha, D.K., Huddleston, S.J., Witkin, J.W., and Baldini, G. (1999). Role of the cysteine-rich domain of the t-SNARE component, SYNDET, in membrane binding and subcellular localization. J. Biol. Chem. *274*, 9053–9060.

Mackler, J.M., Drummond, J.A., Loewen, C.A., Robinson, I.M., and Reist, N.E. (2002). The C_2B Ca^{2+}-binding motif of synaptotagmin is required for synaptic transmission *in vivo*. Nature *418*, 340–344.

Nagy, G., Matti, U., Nehring, R.B., Binz, T., Rettig, J., Neher, E., and Sørensen, J.B. (2002). Protein kinase C-dependent phosphorylation of synaptosome-associated protein of 25 kDa at Ser^{187} potentiates vesicle recruitment. J. Neurosci. *22*, 9278–9286.

Parsons, T.D., Coorssen, J.R., Horstmann, H., and Almers, W. (1995). Docked granules, the exocytotic burst, and the need for ATP hydrolysis in endocrine cells. Neuron *15*, 1085–1096.

Puffer, E.B., Lomneth, R.B., Sarkar, H.K., and Singh, B.R. (2001). Differential role of developmentally distinct SNAP-25 isoforms in the neurotransmitter release process. Biochemistry *40*, 9374–9378.

Ravichandran, V., Chawla, A., and Roche, P.A. (1996). Identification of a novel syntaxin- and synaptobrevin/VAMP-binding protein, SNAP-23, expressed in non-neuronal tissues. J. Biol. Chem. *271*, 13300–13303.

Rizo, J., and Südhof, T.C. (2002). SNAREs and Munc18 in synaptic vesicle fusion. Nat. Rev. Neurosci. *3*, 641–653.

Scales, S., Finley, M.F.A., and Scheller, R.H. (2001). Fusion without SNAREs? Science *294*, 1015–1016.

Schoch, S., Deák, F., Königstorfer, A., Mozhayeva, M., Sara, Y., Südhof, T.C., and Kavalali, E.T. (2001). SNARE function analyzed in Synaptobrevin/VAMP knockout mice. Science *294*, 1117–1122.

Schulte, A., and Chow, R.H. (1996). A simple method for insulation carbon-fiber microelectrodes using aniodic electrophoretic deposition of paint. Anal. Chem. *68*, 3054–3058.

Shin, O.-H., Rhee, J.-S., Tang, J., Sugita, S., Rosenmund, C., and Südhof, T.C. (2003). Sr^{2+} binding to the Ca^{2+} binding site of the synaptotagmin 1 C_2B domain triggers fast exocytosis without stimulating SNARE interactions. Neuron *37*, 99–108.

Smith, C., Moser, T., Xu, T., and Neher, E. (1998). Cytosolic Ca^{2+} acts by two separate pathways to modulate the supply of release-competent vesicles in chromaffin cells. Neuron *20*, 1243–1253.

Söllner, T., Whiteheart, S.W., Brunner, M., Erdjument-Bromage, H., Geromanos, S., Tempts, P., and Rothman, J.E. (1993). SNAP receptors implicated in vesicle targeting and fusion. Nature *362*, 318–324.

Sørensen, J.B., Matti, U., Wei, S.-H., Nehring, R.B., Voets, T., Ashery, U., Binz, T., Neher, E., and Rettig, J. (2002). The SNARE protein SNAP-25 is linked to fast calcium triggering of exocytosis. Proc. Natl. Acad. Sci. USA *99*, 1627–1632.

Sutton, R.B., Fasshauer, D., Jahn, R., and Brunger, A.T. (1998). Crystal structure of a SNARE complex involved in synaptic exocytosis at 2.4Å resolution. Nature *395*, 347–353.

Voets, T. (2000). Dissection of three Ca^{2+}-dependent steps leading to secretion in chromaffin cells from mouse adrenal slices. Neuron *28*, 537–545.

Voets, T., Neher, E., and Moser, T. (1999). Mechanisms underlying phasic and sustained secretion in chromaffin cells from mouse adrenal slices. Neuron *23*, 607–615.

Voets, T., Moser, T., Lund, P., Chow, R.H., Geppert, M., Südhof, T.C., and Neher, E. (2001a). Intracellular calcium dependence of large dense-core vesicle exocytosis in the absence of synaptotagmin I. Proc. Natl. Acad. Sci. USA *98*, 11680–11685.

Voets, T., Toonen, R.F., Brian, E.C., de Wit, H., Moser, T., Rettig, J., Südhof, T.C., Neher, E., and Verhage, M. (2001b). Munc18-1 promotes large dense-core vesicle docking. Neuron *31*, 581–591.

Vogel, K., and Roche, P.A. (1999). SNAP-23 and SNAP-25 are palmitoylated *in vivo*. Biochem. Biophys. Res. Commun. *258*, 407–410.

Wang, C.T., Grishanin, R., Earles, C.A., Chang, P.Y., Martin, T.F., Chapman, E.R., and Jackson, M.B. (2001). Synaptotagmin modulation of fusion pore kinetics in regulated exocytosis of dense-core vesicles. Science *294*, 1111–1115.

Wang, G., Witkin, J.W., Hao, G., Bankaitis, V.A., Scherer, P.E., and Baldini, G. (1997). Syndet is a novel SNAP-25 related protein expressed in many tissues. J. Cell Sci. *110*, 505–513.

Washbourne, P., Thompson, P.M., Carta, M., Costa, E.T., Mathews, J.R., Lopez-Benditó, G., Molnár, Z., Becher, M.W., Valenzula, C.F., Partridge, L.D., and Wilson, M.C. (2002). Genetic ablation of the t-SNARE SNAP-25 distinguishes mechanisms of neuroexocytosis. Nat. Neurosci. *5*, 19–26.

Yang, B., Gonzalez, L., Jr., Prekeris, R., Steegmaier, M., Advani, R.J., and Scheller, R.H. (1999). SNARE interactions are not selective. J. Biol. Chem. *274*, 5649–5653.

Zhang, W., Kim-Miller, M.J., Fukuda, M., Kowalchyk, J.A., and Martin, T.F.J. (2002). Ca^{2+}-dependent synaptotagmin binding to SNAP-25 is essential for Ca^{2+}-triggered exocytosis. Neuron *34*, 599–611.